RSC Advances

ROYAL SOCIETY
OF CHEMISTRY

www.rsc.org/advances

RSC Advances

COMMUNICATIONS

High Performance Pure Sulfur Honeycomb-like Architectures Synthesized by Cooperative Self-assembly Strategy for the Lithium/Sulfur Battery

Xin Liang,[a] Mohammad Kaiser,[a] Konstantin Konstantinov,[a] Richard Tandiono,[b] Zhaoxiang Wang,[c]
5 Hua-Kun Liu,[a] Shi-Xue Dou [a] and Jiazhao Wang,[*a]

Honeycomb-like pure sulfur architectures were synthesized by a cooperative self-assembly strategy, in which a soft
10 **template is used to form the porous structure. Their electrochemical performance is significantly improved comparing with the commercial sulfur powder and the as-prepared sulfur without honeycomb morphology. There has been no report on using soft template to prepare honeycomb-**
15 **like sulfur particles.**

Clean and efficient energy storage devices are in high demand due to the limited global energy supply, environmental pollution, and the increasing consumption of energy[1, 2]. The rechargeable lithium/sulfur battery has attracted significant attention due to its
20 high theoretical specific capacity and power density[3-8]. Another advantage is that sulfur is abundant in nature, inexpensive and non-toxic[9].

In spite of these considerable advantages, the fabrication of lithium/ sulfur batteries encounters a number of challenges.
25 Sulfur is a highly electrically insulating material, which leads to poor electrochemical accessibility and low utilization of the sulfur in the electrode. The polysulfide anions which are formed as the reaction intermediates are highly soluble in the organic electrolyte solvent, which results in low active material
30 utilization, low coulombic efficiency, and short cycle life of the sulfur electrode[10, 11]. In order to successfully operate the lithium-sulfur battery, the elemental sulfur must be well combined with a strong adsorbent to construct a composite cathode[12-15], so as to reduce the diffusion of lithium polysulfides into the electrolyte[16-]
35 [19]. The most promising adsorption agents for the Li/S battery are porous materials such as porous carbon[4, 12, 15, 20], with which porous structured sulfur-carbon composites are prepared by coating elemental sulfur on the surface of the porous carbon materials. The battery performance of these sulfur-carbon
40 composites has shown significant improvement over elemental sulfur, as the porous structure has the following positive effects towards improving the electrochemical performance [21]: (1) the porous structure absorbs the soluble lithium polysulfides formed during discharge and reduces the dissolution of the active
45 materials into the electrolyte; (2) the porous structure increases the contact surface area between the sulfur and the carbon black, which increases the conductivity of the electrode; (3) the porous

structure electrode has a faster charge transfer process, and thus the electrochemical kinetics of the porous sulfur – porous
50 additive electrode is improved in rechargeable lithium batteries. The previously reported methods used for preparation of sulfur – porous additive composites are quite complicated, however, as well as being time-consuming, costly, not environmentally friendly, and difficult to scale up.
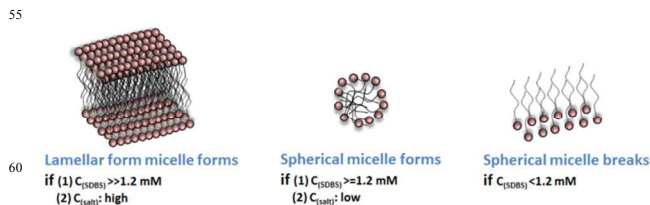55

Figure 1. Different types of SDBS structure in aqueous solution.

It is therefore promising to try to synthesize pure sulfur with
65 porous structure for Li/S batteries. In this study, the sulfur particles with honeycomb morphology were prepared via a cooperative self-assembly process, while sodium dodecyl benzene sulphonate (SDBS) was used as a soft template to form the porous structure. This method is simple, easily scaled up, and
70 has low energy consumption, as shown in Figure S1 in the Supporting Information. SDBS is an excellent soft template to form porous structures[22]. As shown in Figure 1, the structure of SDBS in aqueous solution can easily take on different forms, responding to the concentration of SDBS (C_{SDBS}) and the
75 concentration of salt (C_{salt}) in the solution[22]. When the concentration of SDBS is appropriate, SDBS prefers to form spherical micelles, which are essential to form a porous morphology, and this can be further confirmed by Table S2 and Figure S2. Moreover, SDBS is a non-toxic, biodegradable, and
80 environmentally friendly surfactant. In addition, SDBS is soluble and can be removed after the reaction by using distilled water. To the best of the authors' knowledge, there has been no report on using this method to prepare honeycomb-like sulfur particles. We believe that this method can provide useful guidance for
85 producing high surface area sulfur for various applications, such as in chemical fertilizers, the pharmaceutical industry, the rubber and fibre industries, bioleaching processes, anti-microbial agents, insecticides, fumigants, etc. [23].
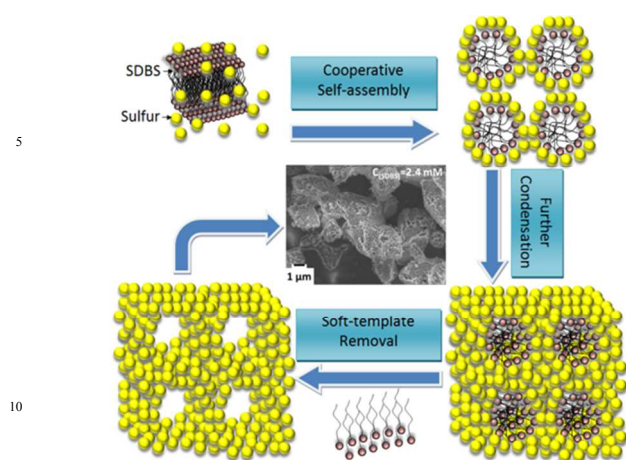
Figure 2. Mechanism of the synthesis of the honeycomb like sulfur particles.

The mechanism of the pore formation is shown in Figure 2. First, after dropping $H_2C_2O_4$ solution into $Na_2S_2O_3$ and SDBS solution, the SDBS lamellar micelles are transformed to spherical micelles as the concentrations of SDBS and salt decrease. At the same time, the sulfur starts to precipitate. Thus, cooperative self-assembly occurs between the sulfur and the SDBS spherical micelles. Then, many more sulfur particles are produced, resulting in further condensation. Secondly, after adding a large amount of H_2O into the above solution, the SDBS spherical micelles break, and the SDBS is removed. The sulfur particles with porous honeycomb-like structure are then finally obtained.

Fig. 3(a) shows the XRD pattern of the prepared sulfur particles. The diffraction peaks can be indexed to the structure of space group Fddd (JCPDS No. 00-008-0247). Fig. 3(b) shows a field emission scanning electron microscope (FESEM) image of the as-prepared sulfur particles with SDBS. It is clear that the morphology is a porous, honeycomb like structure. Fig. 3(c) shows that the sulfur particles without any pores are agglomerated when SDBS is absent. Thus, the SDBS is a critical factor for obtaining the porous sulfur particles. The comparative experiments with different starting concentrations of SDBS were carried out, and it was found that the optimum starting concentration of SDBS was 2.4 mM as shown in Table S1 and Fig. S2. The SEM image of the commercial sulfur powder in Fig. 3(d) shows that the commercial S particles have big particle size and smooth surfaces.

The Brunauer-Emmett-Teller (BET) tests have shown that the specific surface area of the commercial sulfur powder is 0.2023 m^2 g^{-1}, whereas the specific surface area of the as-prepared honeycomb-like sulfur is 1.0990 m^2 g^{-1}, which is about 5 times higher than that of the commercial sulfur powder.

The electrochemical performances of the honeycomb-like sulfur and the commercial sulfur particles were investigated. See the Supporting Information for details of the electrode and cell fabrication. Typical cyclic voltammograms (CV) of the porous sulfur electrode are shown in Fig. 4(a). In the first cycle, there are two main reduction peaks at around 2.4 and 1.8 V, and a small and broad peak near 2.1 V is also observed. The peak near 2.4 V corresponds to the reduction of elemental sulfur to higher-order lithium polysulfides (Li_2S_n, n ⩾ 8). The peak near 1.8 V can be

assigned to the reduction from polysulfides to Li_2S. The small and broad peak near 2.1 V is related to the reduction of higher-order lithium polysulfides (Li_2S_8) to form lower-order lithium polysulfides, such as Li_2S_6 and Li_2S_4 [8], which are agreed well with the charge-discharge curve shown in Fig. S3. Compared to the first cycle, the reduction peaks in the following cycles are shifted slightly to higher voltage because the electrochemical reaction during the first discharge process has to overcome the strong absorbing energy between the sulfur and the conductive matrix[24]. From the second cycle, the intensity of the two oxidation peaks increases with cycling, which indicates that the lithium ion insertion/extraction into sulfur is an activated process[25]. Fig. 4(b) shows the cycling performance of the honeycomb-like sulfur electrode. The potential range of 1.5–3.0 V was selected for the continuous charge–discharge cycling process. During the first 10 cycles, the specific discharge capacity of the honeycomb-like sulfur electrode increased from 696.9 mAh g^{-1} to 816.9 mAh g^{-1}. These results are in good agreement with the CV measurements because of the activation process due to the gradual penetration of the electrolyte into the porous electrode. The discharge specific capacity slightly decreased after 10 cycles. The cells retained a reversible discharge capacity higher than 650 mAh g^{-1} for 50 cycles, while the discharge capacity of the commercial sulfur is only about 200 mAh g^{-1}. It is interesting that the discharge capacity of the initial cycle of the as-prepared sulfur ($C_{(SDBS)}$=0 mM) electrode is as high as 1058 mAh g^{-1}. It can be ascribed to the small particle size of the as-prepared sulfur ($C_{(SDBS)}$=0 mM) particles. The sulfur particle can be mixed very well with carbon black, thus the usage of the sulfur in the initial cycle is very high. But it is also very clearly that the capacity decay is dramatically due to the non-porous structure. The cell with the honey-comb like Sulfur electrode presents improved cycling stability due to the following reasons mentioned in the introduction in relation to the sulfur – porous carbon composite: reduction of the dissolution of the active materials into the electrolyte, increased conductivity of the electrode, and improvement of the kinetics of the Li ion reaction with S.
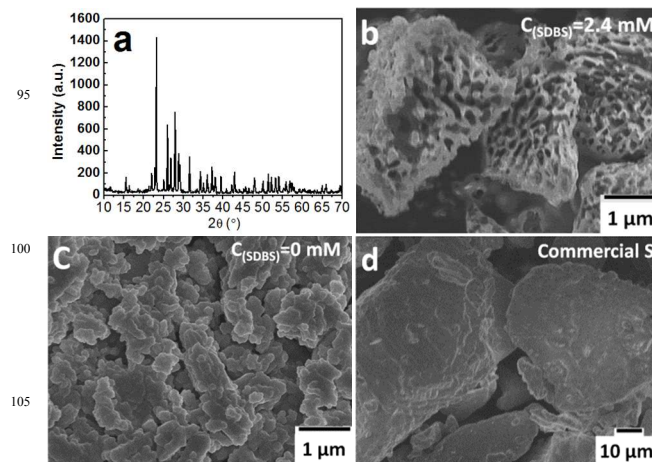

Figure 3. (a) XRD pattern of the sulphur particles; (b) FESEM image of as-prepared honeycomb-like sulfur made with SDBS at high magnification; (c) FESEM image of as-prepared sulfur particles without SDBS; (d) FESEM image of commercial sulfur particles.

In order to verify that the porous structure is responsible for the good performance of the Li/S cell, electrochemical impedance spectroscopy (EIS) measurements were carried out on the commercial Sulfur, as-prepared Sulfur ($C_{(SDBS)}$=0 mM) and honeycomb-like Sulfur electrodes after 5 cycles (Fig. 4(c)). The cell containing honeycomb-like Sulfur shows smaller charge-transfer resistance than the cell with as-prepared Sulfur ($C_{(SDBS)}$=0 mM) electrode and especially the cell with commercial S electrode. Thus, the electrochemical kinetics of the honeycomb-like sulfur has been improved in rechargeable lithium batteries. Figure 4 (d) shows the FESEM image of the honeycomb-like sulfur electrode after 50 cycles. It is clearly that the honeycomb morphology has maintained in the electrode film during cycling. A comparison of the rate capability between the honeycomb-like sulfur electrode and the commercial sulfur electrode is shown in Figure S4. And the effect of the electrolyte has also been discussed in Figure S5.
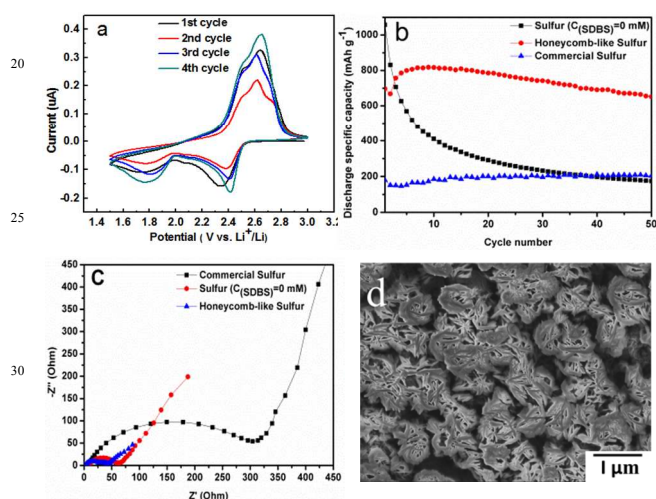

Figure 4. (a) Cyclic voltammograms for the first 4 cycles of the honeycomb-like sulfur electrode; (b) cycling performances of the honeycomb-like sulfur electrode, as-prepared sulfur ($C_{(SDBS)}$=0 mM) electrode and the commercial sulfur electrode; (c) impedance plots for the honeycomb-like sulfur electrode, as-prepared sulfur (C(SDBS)=0 mM) electrode and the commercial sulfur electrode; (d) FESEM image of the honeycomb-like sulfur electrode after 50 cycles

In summary, sulfur particles with honeycomb-like morphology were prepared via a cooperative self-assembly process. The batteries fabricated from the as-prepared honeycomb-like sulfur cathode without any extra adsorption additives show significantly improved electrochemical performance compared with the batteries using commercial sulfur powder and even the as-prepared sulfur without honeycomb-like morphology. The cells with the honeycomb-like sulfur electrode retained a reversible discharge capacity higher than 650 mAh g^{-1} for 50 cycles, while the discharge capacity of the commercial sulfur electrode was about 200 mAh g^{-1}. Moreover, the honeycomb morphology is stable and can be maintained during cycling.

Notes and references

^{a} *Institute for Superconducting and Electronic Materials, University of Wollongong, NSW 2519, Australia. Fax: +61 2 4221 5731; Tel: +61 2 4298 1478; E-mail: jiazhao@uow.edu.au*
^{b} *PT NIPRESS Tbk, J1.Raya Narogong KM. 26 Cileungsi, Bogor 16820 Indonesia*
^{c} *Laboratory for Solid State Ionics, Institute of Physics, Chinese Academy of Sciences, PO Box 603, Beijing 100190, P. R. China*

† Electronic Supplementary Information (ESI) available: [experimental details, diagram of the synthesis process, table of parameters for comparative experiments, FESEM figures of the comparison experiment products,charge/discharge curve of Honeycomb-like sulfur cathode, a comparison of the rate capability between the honeycomb-like sulfur electrode and the commercial sulfur electrode, rate capabilities of honeycomb-like sulfur electrode in different electrolyte]. See DOI: 10.1039/b000000x/

1. L. Wang, X. He, J. Li, J. Gao, J. Guo, C. Jiang and C. Wan, *J. Mater. Chem.*, 2012, **22**, 22077-22081.

2. Y. Deng, Z. Li, Z. Shi, H. Xu, F. Peng and G. Chen, *RSC Adv.*, 2012, **2**, 4645-4647.

3. L. Yin, J. Wang, X. Yu, C. W. Monroe, Y. NuLi and J. Yang, *Chem. Commun.*, 2012, **48**, 7868-7870.

4. X. L. Ji, K. T. Lee and L. F. Nazar, *Nat. Mater.*, 2009, **8**, 500-506.

5. H. L. Wang, Y. Yang, Y. Y. Liang, J. T. Robinson, Y. G. Li, A. Jackson, Y. Cui and H. J. Dai, *Nano Lett.*, 2011, **11**, 2644-2647.

6. J. Wang, J. Chen, K. Konstantinov, L. Zhao, S. H. Ng, G. X. Wang, Z. P. Guo and H. K. Liu, *Electrochim. Acta*, 2006, **51**, 4634-4638.

7. N. W. Li, M. B. Zheng, H. L. Lu, Z. B. Hu, C. F. Shen, X. F. Chang, G. B. Ji, J. M. Cao and Y. Shi, *Chem. Commun.*, 2012, **48**, 4106-4108.

8. L. W. Ji, M. M. Rao, H. M. Zheng, L. Zhang, Y. C. Li, W. H. Duan, J. H. Guo, E. J. Cairns and Y. G. Zhang, *J. Am. Chem. Soc.*, 2011, **133**, 18522-18525.

9. M.-S. Song, S.-C. Han, H.-S. Kim, J.-H. Kim, K.-T. Kim, Y.-M. Kang, H.-J. Ahn, S. X. Dou and J.-Y. Lee, *J. Electrochem. Soc.*, 2004, **151**, A791-A795.

10. B. Zhang, X. Qin, G. R. Li and X. P. Gao, *Energy Environ. Sci.*, 2010, **3**, 1531-1537.

11. M. Nagao, A. Hayashi and M. Tatsumisago, *Electrochim. Acta*, 2011, **56**, 6055-6059.

12. J. Wang, S. Y. Chew, Z. W. Zhao, S. Ashraf, D. Wexler, J. Chen, S. H. Ng, S. L. Chou and H. K. Liu, *Carbon*, 2008, **46**, 229-235.

13. X. Ji, K. T. Lee and L. F. Nazar, *Nat Mater*, 2009, **8**, 500-506.

14. J.-Z. Wang, L. Lu, M. Choucair, J. A. Stride, X. Xu and H.-K. Liu, *J. Power Sources*, 2011, **196**, 7030-7034.

15. N. Jayaprakash, J. Shen, S. S. Moganty, A. Corona and L. A. Archer, *Angew. Chem. Int. Ed.*, 2011, **123**, 6026-6030.

16. X. L. Ji and L. F. Nazar, *J. Mater. Chem.*, 2010, **20**, 9821-9826.

17. Z. Wei Seh, W. Li, J. J. Cha, G. Zheng, Y. Yang, M. T. McDowell, P.-C. Hsu and Y. Cui, *Nat. Commun.*, 2013, **4**, 1331-1331.

18. S. Evers, T. Yim and L. F. Nazar, *J. Mater. Chem. C*, 2012, **116**, 19653-19658.

19. Y. J. Choi, B. S. Jung, D. J. Lee, J. H. Jeong, K. W. Kim, H. J. Ahn, K. K. Cho and H. B. Gu, *Phys. Scr.*, 2007, **T129**, 62-65.

20. C. Lai, X. P. Gao, B. Zhang, T. Y. Yan and Z. Zhou, *J. Phys. Chem. C*, 2009, **113**, 4712-4716.

21. W. Yuan, D. Xie, Z. Dong, Q. Su, J. Zhang, G. Du and B. Xu, *Mater. Lett.*, 2013, **97**, 129-132.

5 22. N. Pal and A. Bhaumik, *Adv.Colloid and Interface Sci.*, 2013, **189**, 21-41.

23. Y. M. Guo, J. Z. Zhao, S. F. Yang, Z. C. Wang and H. B. Zhang, *Powder Technol.*, 2006, **162**, 83-86.

24. X. Liang, Z. Wen, Y. Liu, H. Zhang, J. Jin, M. Wu and X. Wu, *J. Power Sources*, 2012, **206**, 409-413.

25. X. Liang, Z. Wen, Y. Liu, H. Zhang, L. Huang and J. Jin, *J. Power Sources*, 2011, **196**, 3655-3658.